J Neurooncol (2012) 108:469–475
DOI 10.1007/s11060-012-0840-5

CLINICAL STUDY

# [18F]-Fluorodeoxyglucose positron emission tomography in children with neurofibromatosis type 1 and plexiform neurofibromas: correlation with malignant transformation

**L. L. Tsai · L. Drubach · F. Fahey · M. Irons · S. Voss · N. J. Ullrich**

Received: 3 October 2011 / Accepted: 20 February 2012 / Published online: 11 March 2012


**Abstract** The objective of this study was to investigate the predictive value of [18F]-fluorodeoxyglucose positron emission tomography (FDG-PET) in detecting malignant transformation of plexiform neurofibromas in children with neurofibromatosis type 1 (NF1). An electronic search of the medical records was performed to determine patients with NF1 who had undergone FDG-PET for plexiform neurofibroma between 2000 and 2011. All clinical, radiologic, pathology information and operative reports were reviewed. Relationship between histologic diagnosis, radiologic features and FDG-PET maximum standardized uptake value ($SUV_{max}$) was evaluated. This study was approved by the Institutional Review Board of our institution. 1,450 individual patients were evaluated in our Multidisciplinary Neurofibromatosis Program, of whom 35 patients underwent FDG-PET for suspected MPNST based on change or progression of clinical symptoms, or MRI findings suggesting increased tumor size. Twenty patients had concurrent pathologic specimens from biopsy/excision of 27 distinct lesions (mean age 14.9 years). Pathologic interpretation of these specimens revealed plexiform and atypical plexiform neurofibromas ($n = 8$ each), low grade MPNST ($n = 2$), intermediate grade MPNST ($n = 4$), high grade MPNST ($n = 2$), GIST ($n = 1$) and non-ossifying fibroma ($n = 1$). $SUV_{max}$ of plexiform neurofibromas (including typical and atypical) was significantly different from MPNST (2.49 (SD = 1.50) vs. 7.63 (SD = 2.96), $p < 0.001$). A cutoff $SUV_{max}$ value of 4.0 had high sensitivity and specificity of 1.0 and 0.94 to distinguish between PN and MPNST. FDG-PET can be helpful in predicting malignant transformation in children with plexiform neurofibromas and determining the need for biopsy and/or surgical resection.

**Keywords** Neurofibromatosis type 1 · Plexiform neurofibroma · Malignant peripheral nerve sheath tumor · Transformation · PET

L. L. Tsai · L. Drubach · F. Fahey · S. Voss
Department of Radiology, Children's Hospital Boston, 300 Longwood Avenue, Boston, MA 02115, USA

L. L. Tsai
Department of Radiology, Beth Israel Deaconess Medical Center, Boston, MA, USA

L. Drubach · F. Fahey
Department of Nuclear Medicine, Children's Hospital Boston, 300 Longwood Avenue, Boston, MA 02115, USA

M. Irons
Department of Medicine, Children's Hospital Boston, 300 Longwood Avenue, Boston, MA 02115, USA

N. J. Ullrich (✉)
Department of Neurology, Children's Hospital Boston, 300 Longwood Avenue, Boston, MA 02115, USA
e-mail: nicole.ullrich@childrens.harvard.edu

## Introduction

Neurofibromatosis 1 (NF1) is a common autosomal dominant disorder, with an incidence of one in 3,500 live births [1, 2]. Individuals with NF1 are at risk to develop benign and malignant tumors; the leading cause of mortality among these individuals is the development of malignant peripheral nerve sheath tumors (MPNST). The lifetime risk of MPNST in patients with NF1 is 8–13% and prognosis is poor, with a five-year overall survival of 21–41% [3].

MPNST typically results from malignant degeneration of benign NF1 lesions, including plexiform neurofibromas

(PN) and subcutaneous neurofibromas [4, 5]. The presence of a PN elevates the risk of MPNST formation by 20-fold amongst NF1 patients [6]. The ability to identify predictors of PN progression, therefore, is important for diagnostic and therapeutic purposes. Clinical features suggestive of malignancy include unremitting pain and/or a rapid increase in the size or consistency, or development of new neurologic deficit [7]. Lesions are often followed with MRI, CT, or [$^{18}$F]-fluorodeoxyglucose (FDG) PET. The gold standard method of differentiation between PN and MPNST is by pathologic evaluation after biopsy or excision.

FDG-PET imaging is able to identify areas of high glucose metabolism throughout the body [8–10]. A number of studies using FDG-PET in adults with NF1 have demonstrated a significant difference in mean standardized uptake values (SUV) between benign and malignant lesions [11–13].

The objective of this study was to obtain correlative imaging and pathology to investigate the predictive value of FDG-PET in detecting malignant transformation of PN and to distinguish benign from malignant tumors in children with NF1. We hypothesize that the wider variability in growth rates of these tumors in children may result in a greater spectrum of FDG-avidity that can further differentiate between benign and malignant tumors.

## Materials and methods

### Study population

This retrospective, HIPPA-compliant study was approved by the Institutional Review Board of our institution with waiver of individual consent. An electronic search engine using Boolean operators and combinations of the key words NF1/neurofibromatosis, PET, PN and MPNST was used to identify subjects with NF1, less than 21 years of age, who were evaluated at the Multidisciplinary Neurofibromatosis Program at Children's Hospital Boston and Dana-Farber Cancer Institute between 2000 and 2011 and who had also undergone FDG-PET evaluations for PN or MPNST. Only those patients who had undergone subsequent biopsy or resection were included. All patients met the clinical criteria for NF1 [2].

Data collection included demographic information, dates of initial imaging that showed the abnormality, indication for MRI and FDG-PET scans, and pathology. Clinical data detailing the physical, neurological and neuropathologic examinations were reviewed. Lesions were classified as typical neurofibroma, atypical neurofibroma, or MPNST. Atypical neurofibroma was defined as neurofibroma exhibiting nuclear atypia and/or hypercellularity, without mitoses or necrosis [14, 15]. MPNST were classified as low, intermediate or high grade depending on degree of tumor differentiation, vascular invasion, necrosis and number of mitoses [16].

### Imaging studies

MRI studies were obtained using a 1.5-Tesla unit (GE Medical Systems). The MRI protocol included multiplanar conventional T1-weighted images, T2-weighted, sagittal T1-weighted, axial T2-weighted, fluid attenuated (FLAIR) and fat-suppressed (FSEIR) inversion recovery, and multiplanar gadolinium-enhanced fat-suppressed T1-weighted images. We reviewed all available neuroimaging studies to determine the extent of the lesion, presence or absence of enhancement and evidence for radiologic progression.

FDG-PET imaging was performed on a GE Advance Nxi PET scanner (GE Healthcare Technologies, Waukesha, WI, USA). Whole body attenuation corrected images were acquired in 2-dimensional mode, approximately 60 min after intravenous administration of $^{18}$F-FDG (dose 5.55 MBq/kg, minimum 18.5 MBq, and maximum 370 MBq). Images were acquired for 8 min per bed position (5 min emission and 3 min transmission). All patients were instructed to fast for at least 4 h prior to imaging, to refrain from heavy exercise for the prior 24 h and to dress warmly on the day of the test. Blood glucose was measured at time of tracer administration. If glucose values were greater than 200 mg/dL, the study was rescheduled. The maximum standardized uptake value ($SUV_{max}$) was calculated by drawing a region of interest (ROI) in a coronal section of the FDG-PET using a Hermes Hybrid Viewer Gold 3 application (Hermes workstation, Stockholm, Sweden) where a lesion was identified on MR or CT. $SUV_{max}$ was defined as the maximum voxel FDG-PET value, calibrated to the activity concentration within the lesion normalized by the decay-corrected administered activity and the patient's weight. SUV calculations were made by a nuclear physician (LD) who was blinded to the clinical history and pathological results.

Several imaging studies were imported from external institutions, as our institution was a local tertiary referral center for NF1 patients with PN. In these cases, the raw data for each PET examination was used to recalculate $SUV_{max}$ using consistent methods of adjustments to injected dose, tissue tracer concentration, body weight, and serum glucose levels. The $SUV_{max}$ calculations were performed by a nuclear physicist (FF) with ROI marked by the nuclear medicine physician (LD). Both were blinded to the clinical history and pathological results. This allowed us to more reliably compare $SUV_{max}$ between studies performed on different imaging systems.

**Table 1** Subject data and lesion characteristics

| Subject | Age (years) | Gender | Location | Pathology | SUVmax |
|---|---|---|---|---|---|
| 1 | 17 | M | Left arm | PN | 2.70 |
| | | | Right axilla | PN | 3.50 |
| 2 | 15 | F | Sacral mass | APN | 1.50 |
| 3 | 17 | M | Right scalp | PN | 1.70 |
| 4 | 16 | M | Right chest | MPNST-low | 5.10 |
| 5 | 6 | F | Left neck | PN | 2.40 |
| 6 | 17 | F | Right buttock | PN | 1.70 |
| 7 | 10 | M | Right shoulder | APN | 2.57 |
| 8 | 19 | F | Right neck | MPNST-intermediate | 11.70 |
| 9 | 13 | M | Right thigh | APN | 2.52 |
| | | | Thorax, paraspinal | PN | 1.30 |
| 10 | 19 | F | Right arm | PN | 1.20 |
| 11 | 20 | M | Pelvic mass | MPNST-intermediate | 8.36 |
| | | | Pelvic mass | MPNST-intermediate | 4.32 |
| | | | Right abdomen | MPNST-high | 6.70 |
| 12 | 20 | F | Left clavicle | PN | 1.40 |
| 13 | 17 | F | Right chest | MPNST-high | 12.90 |
| 14 | 1 | M | Right lung | MPNST-high | 5.10 |
| 15 | 18 | F | Right ankle | APN | 2.86 |
| 16 | 17 | F | Right thigh | APN | 0.56 |
| 17 | 12 | F | R popliteal fossa | MPNST-intermediate | 7.00 |
| | | | Right tibia | APN | 3.00 |
| | | | Right tibia | APN | 6.90 |
| 18 | 20 | F | Right neck | MPNST-low | 7.47 |
| | | | Right neck | APN | 4.06 |
| 19 | 7 | F | Stomach | GIST | 3.20 |
| 20 | 19 | F | Right femur | NOF | 4.10 |

*PN* plexiform neurofibroma, *APN* atypical plexiform neurofibroma, *MPNST* malignant peripheral nerve sheath tumor, *GIST* gastrointestinal stromal tumor, *NOF* non-ossifying fibroma

### Statistics

The data were analyzed using the statistical database software (JMP, SAS Institute), and dot plots were used to display the distribution of FDG uptake. A student's $t$ test was used to compare $SUV_{max}$ values and histologic diagnosis of PN versus MPNST. $p$ Values $<0.05$ were considered to be statistically significant. Sensitivity and specificity were calculated for several cutoff $SUV_{max}$ values between 3.0 and 5.0. Corresponding binomial proportion confidence intervals for estimated sensitivity and specificity were obtained using the Wilson method.

## Results

A total of 1,450 individual patients were evaluated between 2000 and 2011. There were 35 patients who met clinical criteria for NF1 who had undergone FDG-PET for PN or suspected MPNST based on change or progression of clinical symptoms. Of these, 20 patients had concurrent pathologic specimens from biopsy or excision of 27 distinct FDG-avid lesions (Table 1). One of the lesions did not have an MRI or CT performed near the time of PET imaging; the remaining 26 lesions had cross-sectional imaging performed within 2 months of PET evaluation, with mean and median interval times of 18.0 and 10.0 days, respectively. The mean age of this subset of individuals was 14.9 years (range 1–20) and included 7 males and 13 females. Indications for obtaining PET imaging on these patients included: increased growth rate ($n = 8$), lesional pain ($n = 10$), concern on MR imaging ($n = 5$), worrisome lesion detected after imaging of other index lesion ($n = 2$) and constitutional symptoms (weight loss/cachexia, $n = 1$). Some patients had more than one indication for imaging.

Lesions were present in a wide variety of locations including the head and neck, thorax, pelvis, and extremities

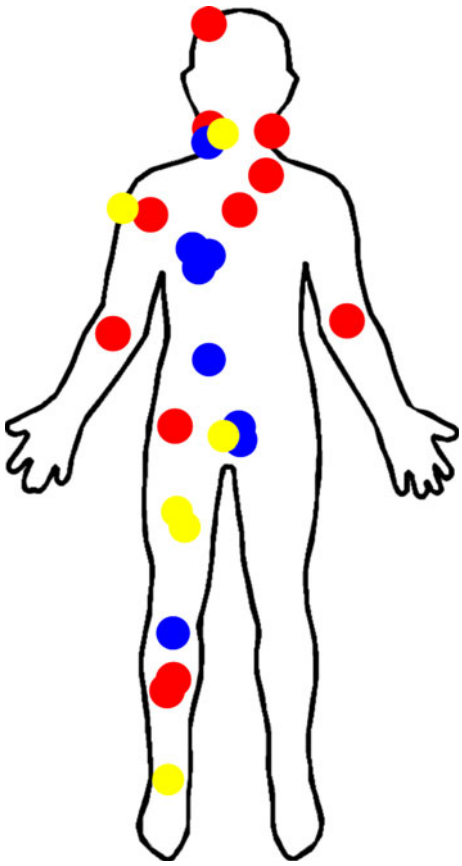

**Fig. 1** Location and laterality of lesions in patient cohort including benign plexiform neurofibroma (*red*), atypical plexiform neurofibroma (*yellow*) and malignant peripheral nerve sheath tumors (*blue*)

(Fig. 1). Only three lesions were left sided. On cross-sectional imaging, PN and MPNST can exhibit similar fusiform shapes, enhance variably with contrast, and on MRI are generally T2 hyperintense. Atypical PN (APN) and PN typically have well-defined borders and appear relatively less heterogeneous on T2-weighted imaging (Fig. 2). When present, characteristics favoring MPNST include ill-defined margins, obscuration of neighboring fat planes suggesting local invasion, and central necrosis (Fig. 3).

The location of the FDG-PET abnormalities in these patients corresponded to those noted on CT and/or MR imaging. PET imaging did not reveal new NF lesions that had not been seen by either CT or MRI. Two outside studies were excluded from SUV analysis because there was a lack of one or more of the adjustment factors for injected dose, body weight or serum glucose. For the remaining 25 samples, $SUV_{max}$ was calculated for all lesions and measurements ranged from 0.56 to 12.9 (mean = 4.34, median = 3.00). When possible, PET images were fused with MR or CT examinations to confirm accurate lesion characterization. A summary of $SUV_{max}$ data is seen in Table 1 and shown graphically in Fig. 4. Two SUV measurements were obtained from an outside hospital report. While the available PET data were insufficient to recalculate and confirm these findings within our department, these data were still included in our analysis.

Pathologic interpretation of the surgical and biopsy specimens revealed PN ($n = 16$), low grade MPNST ($n = 2$), intermediate grade MPNST ($n = 4$), high grade MPNST ($n = 4$), gastrointestinal stromal tumor (GIST, $n = 1$), and non-ossifying fibroma (NOF, $n = 1$). The two patients with GIST and NOF were not included in further analysis. Of the 16 PN specimens, eight were considered typical neurofibroma/PN and eight demonstrated atypical features, including hypercellularity, hyperchromatism, and nuclear enlargement and pleomorphism.

We evaluated the relationship between $SUV_{max}$ and pathology. Benign and APN demonstrated only mildly increased uptake on FDG-PET (Fig. 2), whereas malignant lesions typically demonstrated intense radiotracer uptake (Fig. 3). Based on quantitative analysis of PET data, PN and MPNSTs demonstrated mean maximum SUV of 2.49 (SD = 1.50) and 7.63 (SD = 2.96), respectively, a difference that was statistically significant ($p < 0.001$).

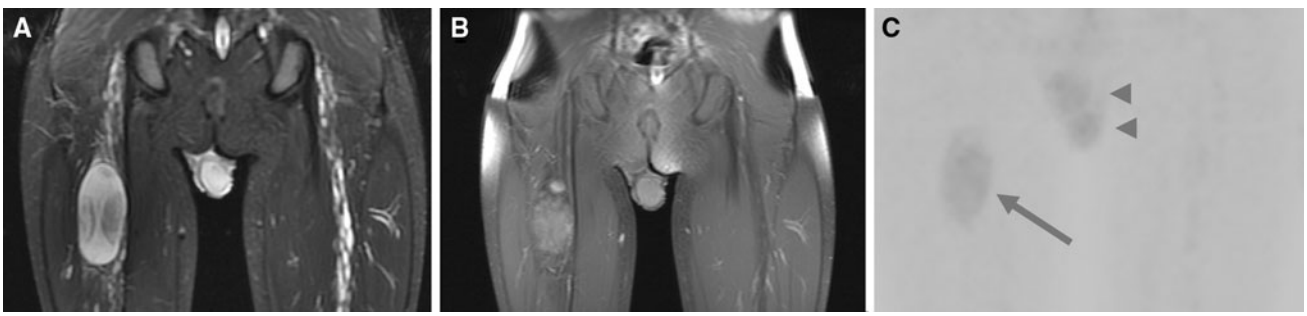


**Fig. 2** Atypical plexiform neurofibroma in a 13 year-old boy with NF1 presenting with increasing thigh circumference. **a** Coronal FSEIR MR imaging demonstrates T2 hyperintense lesions along the neurovascular bundle, consistent with multiple nerve sheath tumors. In addition, there is a dominant focal lesion in the proximal right thigh, which demonstrates modest enhancement on T1-post contrast imaging (**b**). **c** Coronal whole-body FDG PET imaging shows focal area of increased $^{18}$F-FDG uptake in the dominant tumor (*arrow*, $SUV_{max} = 2.52$). Two neighboring foci of tracer activity represent physiological uptake within the testicles (*arrowheads*)

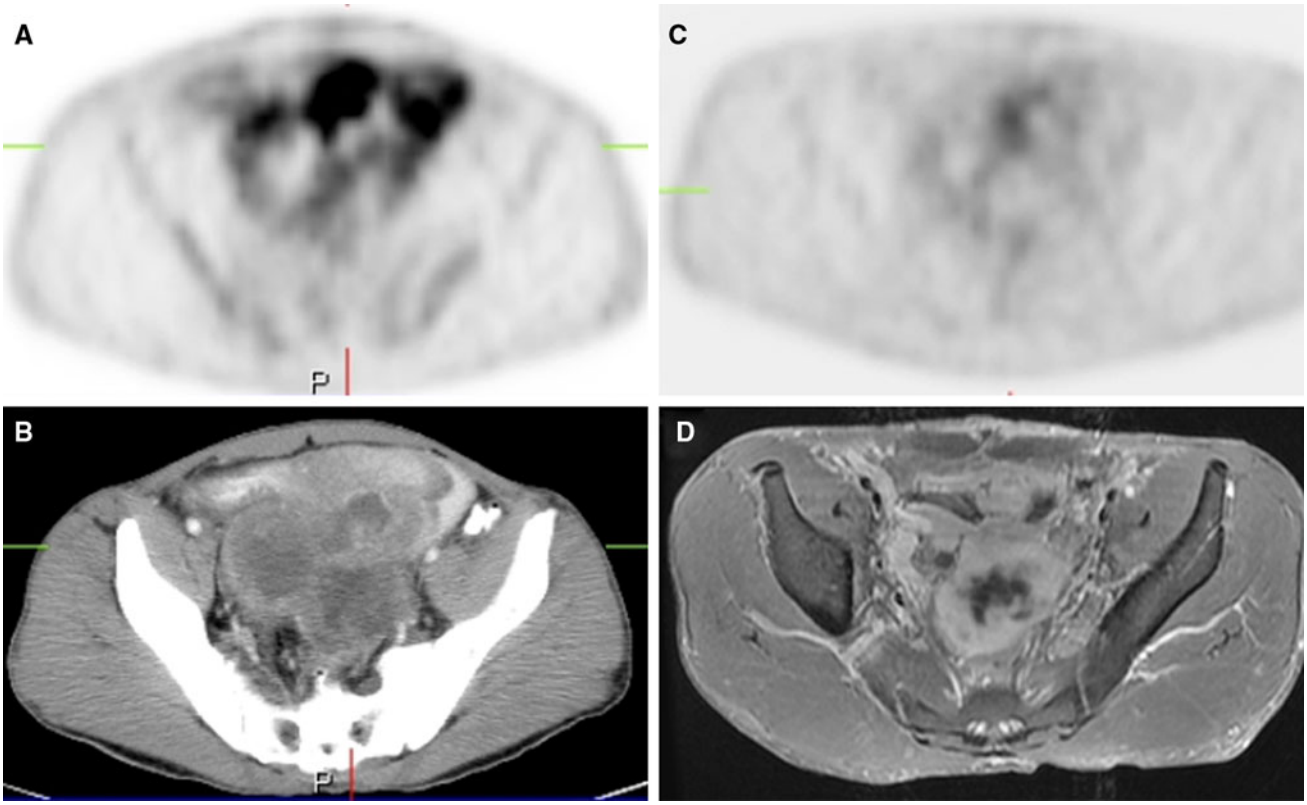


**Fig. 3** MPNST in a 20 year old male with NF1 demonstrating interval decrease in FDG uptake following surgery and chemoradiation. The patient initially presented with pallor, fatigue, abdominal pain, and weight loss. Pre-treatment PET (**a**) and CT (**b**) images demonstrate a highly FDG-avid pelvic mass ($SUV_{max} = 8.36$), consistent with intermediate grade MPNST on pathology. PET performed 3 months later for progressive symptoms on treatment demonstrates (**c**) decreased but elevated FDG-avidity of the main mass ($SUV_{max} = 4.32$). T1-weighted post-contrast MRI (**d**) shows an ill-defined multilobulated enhancing mass with central non-enhancing regions likely reflecting areas of necrosis

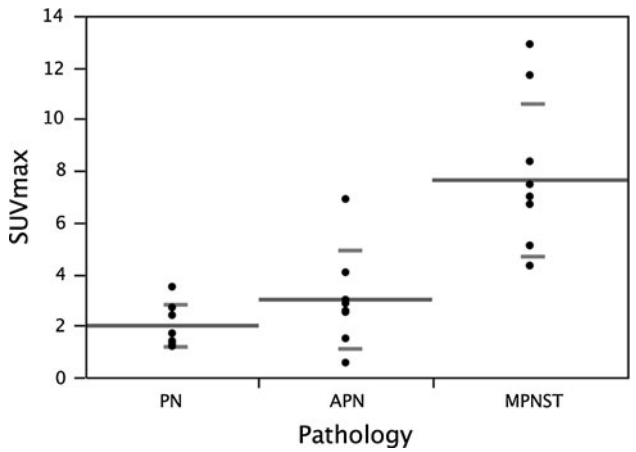


**Fig. 4** Comparison of $SUV_{max}$ between neurofibromas (PN), atypical neurofibromas (APN) and all MPNSTs. The mean (*long line*) and standard deviation (*short line*) for each subgroup are shown

When neurofibromas were separated into PN and APN, there was no significant difference between subgroups: PN and APN demonstrated mean $SUV_{max}$ of 1.99 (SD = 0.81) and 3.00 (SD = 1.89), respectively ($p = 0.35$). Both subtypes, however, demonstrated mean $SUV_{max}$ values significantly different from MPNST ($p < 0.001$ for each).

The sensitivity and specificity for distinguishing between PN and MPNST were determined at $SUV_{max}$ values of 3.0, 4.0, and 5.0. Sensitivity and specificity at $SUV_{max}$ of 3.0 were 1.0 (95% CI [0.7, 1.0]) and 0.81 (CI [0.57, 0.93]), at $SUV_{max}$ of 4.0 were 1.0 (CI [0.7, 1.0]) and 0.94 (CI [0.71–0.99]), and at $SUV_{max}$ of 5.0 were 0.89 (CI [0.57, 0.98]) and 0.94 (CI [0.71, 0.99]. This suggests an optimal cutoff of 4.0 as the $SUV_{max}$ that best predicts malignant transformation.

## Discussion

The major cause of morbidity in patients with NF1 is the transformation of a PN into an MPNST. Both PN and MPNST can have a variable appearance on conventional cross-sectional imaging, a finding that correlates well to their highly heterogeneous histological appearance [17, 18]. Growth rates can also vary in PN, and some lesions may demonstrate rapid growth while

others grow slowly, even with periods of relative quiescence [19].

MRI alone can detect malignant degeneration into MPNST, but with modest sensitivity, particularly when tumors exhibit internal lobular features and high T1-weighted signal intensity [18]. MRI, however, cannot be used to predict which tumors are likely to progress. Early radiologic indicators are crucial to predict which tumors are more likely to be malignant, which might require biopsy or surgical excision, and which are recurrent.

Our data support the hypothesis that benign and malignant lesions are distinguishable by FDG-PET imaging and that there is a correlation between mean $SUV_{max}$ and tumor grade in children with NF1. The most marked difference was between benign/atypical neurofibromas and MPNSTs. It is of note that there was no significant difference in mean $SUV_{max}$ between benign and atypical neurofibromas. However, $SUV_{max}$ values for APN lesions overlapped with those of benign PN and MPNST, whereas there was no overlap when comparing only benign PN against MPNST. This may reflect sampling variability and the spectrum of pathological changes that occur in the transition from benign to atypical neurofibroma to low grade MPNST. Similar findings were also suggested on a prior study with a study population mainly consisting of adults [13].

Clinico–radiologic–pathologic correlations of PN and MPNST have been evaluated in adults, but there is limited data in children. FDG-PET is currently recommended only when there has been a significant interval change in tumor size on followup imaging, or if the clinical history is suspicious for malignancy. One study demonstrated that FDG-PET is sensitive (95%) but less specific (72%) for MPNST, with improved specificity using concurrent $^{11}$C-methionine PET [20]. Another case series in adults used FDG-PET in PN suspicious for malignant change and found a significant difference in mean SUV between the malignant and benign tumors [13, 21]. A prospective study of FDG-PET in children and young adults with PN without concerning clinical or radiologic features at study entry demonstrated a correlation between subsequent change in PN volume and progressive increased FDG uptake, although correlative pathology was not available [11]. Lastly, there is one recent study of surveillance FDG-PET in children with optic pathway gliomas and PN, but with limited correlative pathology; in the two patients who underwent biopsy for SUV >4, pathology demonstrated MPNST [22].

In our study, increased SUV was able to distinguish between biopsy-confirmed PN and MPNST, with a range of SUV values that are comparable to those reported in the largest adult series. In prior studies, an $SUV_{max}$ cutoff of 3 was shown to discriminate between benign and malignant lesions in adults, although there was a range of $SUV_{max}$ values (2.7–4.0) where overlap existed between benign and malignant tumors [10, 12, 13, 20, 23, 24]. FDG-PET, however, may be falsely-negative in some malignant lesions [25]. In our study, $SUV_{max}$ of 4.0 could be used as a cutoff to distinguish between benign and malignant tumors with high sensitivity and specificity. This suggests that a combination of FDG-PET and MRI may allow us to accurately determine which lesions are at greatest risk of malignant transformation. Thus, FDG-PET may be an important correlative imaging modality for evaluation and follow-up of clinically and/or radiologically suspicious lesions. There may also be a role for FDG-PET following surgery or to determine response to treatment for MPNST as well as to detect disease recurrence. Whether FDG-PET should be used in routine screening of asymptomatic PN in an effort to detect occult MPNST remains to be determined.

Management of PN in the pediatric population is particularly challenging, as PN growth can be more rapid during early childhood and later in adolescence, further raising concern for malignant progression. In addition, head and neck PN, which are more frequent in children, are also less surgically accessible; interventions are considered only if there is significant neurological impairment or concern for malignant transformation. Concerns about ionizing radiation exposure also limit use of CT for routine examinations. However, MRI examinations are often lengthy and may require sedation or anesthesia. Despite these challenges, this study demonstrates that combination of FDG-PET and MR or CT imaging may help to identify degeneration of PN to MPNST; MR and CT are crucial for precise anatomical localization, lesion localization and interpretation of FDG-PET data. To our knowledge this is the first study in the pediatric population that includes concurrent clinico–pathologic–radiologic analysis of peripheral nerve sheath tumors and suggests that FDG-PET may also assist in predicting tumor grade.

Our study had several limitations. Many patients were referred for multidisciplinary consultation from outside institutions and cases where pathology was not available were not included. In addition, long-term followup was not possible in some patients. The time interval between FDG-PET imaging and biopsy ranged from under 1 week to 4 months. Since transformation of PN to MPNST is unidirectional, we may have included MPNST that were PN during prior MR or FDG-PET imaging; however, the natural history of neurofibromas suggests that it is unlikely that malignant transformation occurred between FDG-PET and biopsy.

In conclusion, our data support the hypothesis that FDG-PET may be useful to help distinguish between benign and malignant lesions in children with NF1 and further support a correlation between mean $SUV_{max}$ and tumor grade. Optimal management of PN in children with NF1 depends on

early and accurate detection of malignant transformation using reliable imaging techniques that provide correlative information regarding tumor metabolism, particularly in situations where biopsy or excision is associated with high risk. Ultimately, FDG-PET may be useful as an adjunct to traditional imaging to help predict early treatment response and disease remission. As new radionucleotide tracers become available, this may further help provide prognostic information regarding tumor grade.

**Conflict of interest**

The authors declare that they have no conflict of interest.

## References


1. Listernick R, Charrow J (1990) Neurofibromatosis type 1 in childhood. J Pediatr 116:845–853
2. National Institutes of Health Concensus Development Conference Statement: neurofibromatosis (1988) Neurofibromatosis 1:172–178
3. Widemann BC (2009) Current status of sporadic and neurofibromatosis type 1-associated malignant peripheral nerve sheath tumors. Curr Oncol Rep 11:322–328
4. Brems H, Beert E, de Ravel T, Legius E (2009) Mechanisms in the pathogenesis of malignant tumours in neurofibromatosis type 1. Lancet Oncol 10:508–515
5. Gottfried ON, Viskochil DH, Couldwell WT (2010) Neurofibromatosis type 1 and tumorigenesis: molecular mechanisms and therapeutic implications. Neurosurg Focus 28:E8
6. Tucker T, Wolkenstein P, Revuz J, Zeller J, Friedman JM (2005) Association between benign and malignant peripheral nerve sheath tumors in NF1. Neurology 65:205–211
7. Ferner RE, Gutmann DH (2002) International consensus statement on malignant peripheral nerve sheath tumors in neurofibromatosis. Cancer Res 62:1573–1577
8. Hoh CK, Hawkins RA, Glaspy JA, Dahlbom M, Tse NY, Hoffman EJ, Schiepers C, Choi Y, Rege S, Nitzsche E et al (1993) Cancer detection with whole-body PET using 2-[18F] fluoro-2-deoxy-D-glucose. J Comput Assist Tomogr 17:582–589
9. Wong TZ, van der Westhuizen GJ, Coleman RE (2002) Positron emission tomography imaging of brain tumors. Neuroimaging Clin N Am 12:615–626
10. Cardona S, Schwarzbach M, Hinz U, Dimitrakopoulou-Strauss A, Attigah N (2003) Mechtersheimer section sign G, Lehnert T: evaluation of F18-deoxyglucose positron emission tomography (FDG-PET) to assess the nature of neurogenic tumours. Eur J Surg Oncol 29:536–541
11. Fisher MJ, Basu S, Dombi E, Yu JQ, Widemann BC, Pollock AN, Cnaan A, Zhuang H, Phillips PC, Alavi A (2008) The role of [18F]-fluorodeoxyglucose positron emission tomography in predicting plexiform neurofibroma progression. J Neurooncol 87:165–171
12. Brenner W, Friedrich RE, Gawad KA, Hagel C, von Deimling A, de Wit M, Buchert R, Clausen M, Mautner VF (2006) Prognostic relevance of FDG PET in patients with neurofibromatosis type-1 and malignant peripheral nerve sheath tumours. Eur J Nucl Med Mol Imaging 33:428–432
13. Ferner RE, Golding JF, Smith M, Calonje E, Jan W, Sanjayanathan V, O'Doherty M (2008) [18F]2-fluoro-2-deoxy-D-glucose positron emission tomography (FDG PET) as a diagnostic tool for neurofibromatosis 1 (NF1) associated malignant peripheral nerve sheath tumours (MPNSTs): a long-term clinical study. Ann Oncol 19:390–394
14. Valeyrie-Allanore L, Ortonne N, Lantieri L, Ferkal S, Wechsler J, Bagot M, Wolkenstein P (2008) Histopathologically dysplastic neurofibromas in neurofibromatosis 1: diagnostic criteria, prevalence and clinical significance. Br J Dermatol 158:1008–1012
15. Lin BT, Weiss LM, Medeiros LJ (1997) Neurofibroma and cellular neurofibroma with atypia: a report of 14 tumors. Am J Surg Pathol 21:1443–1449
16. van Vliet M, Kliffen M, Krestin GP, van Dijke CF (2009) Soft tissue sarcomas at a glance: clinical, histological, and MR imaging features of malignant extremity soft tissue tumors. Eur Radiol 19:1499–1511
17. Spurlock G, Knight SJ, Thomas N, Kiehl TR, Guha A, Upadhyaya M (2010) Molecular evolution of a neurofibroma to malignant peripheral nerve sheath tumor (MPNST) in an NF1 patient: correlation between histopathological, clinical and molecular findings. J Cancer Res Clin Oncol 136:1869–1880
18. Matsumine A, Kusuzaki K, Nakamura T, Nakazora S, Niimi R, Matsubara T, Uchida K, Murata T, Kudawara I, Ueda T, Naka N, Araki N, Maeda M, Uchida A (2009) Differentiation between neurofibromas and malignant peripheral nerve sheath tumors in neurofibromatosis 1 evaluated by MRI. J Cancer Res Clin Oncol 135:891–900
19. Korf BR (1999) Plexiform neurofibromas. Am J Med Genet 89:31–37
20. Bredella MA, Torriani M, Hornicek F, Ouellette HA, Plamer WE, Williams Z, Fischman AJ, Plotkin SR (2007) Value of PET in the assessment of patients with neurofibromatosis type 1. AJR Am J Roentgenol 189:928–935
21. Warbey VS, Ferner RE, Dunn JT, Calonje E, O'Doherty MJ (2009) [18F] FDG PET/CT in the diagnosis of malignant peripheral nerve sheath tumours in neurofibromatosis type-1. Eur J Nucl Med Mol Imaging 36:751–757
22. Moharir M, London K, Howman-Giles R, North K (2010) Utility of positron emission tomography for tumour surveillance in children with neurofibromatosis type 1. Eur J Nucl Med Mol Imaging 37:1309–1317
23. Basu S, Nair N (2006) Potential clinical role of FDG-PET in detecting sarcomatous transformation in von Recklinghausen's disease: a case study and review of the literature. J Neurooncol 80:91–95
24. Karabatsou K, Kiehl TR, Wilson DM, Hendler A, Guha A (2009) Potential role of 18fluorodeoxyglucose-positron emission tomography/computed tomography in differentiating benign neurofibroma from malignant peripheral nerve sheath tumor associated with neurofibromatosis 1. Neurosurgery 65:A160–A170
25. Shahid KR, Amrami KK, Esther RJ, Lowe VJ, Spinner RJ (2011) False-negative fluorine-18 fluorodeoxyglucose positron emission tomography of a malignant peripheral nerve sheath tumor arising from a plexiform neurofibroma in the setting of neurofibromatosis type 1. J Surg Orthop Adv 20:132–135